Osteoarthritis and Cartilage (1999) **7,** 41–58

1063–4584/99/010041+18 $12.00/0
Article No. joca.1998.0161, available online at http://www.idealibrary.com on IDEAL

Osteoarthritis and Cartilage
Journal of the OsteoArthritis Research Society International

The extracellular matrix, interstitial fluid and ions as a mechanical signal transducer in articular cartilage

By Van C. Mow, Christopher C. Wang and Clark T. Hung
Orthopaedic Research Laboratory and Center for Biomedical Engineering, Columbia University, New York, NY 10032

Summary

Objective: (1) Provide an overview of the biomechanical factors that are required to analyze and interpret biological data from explant experiments; (2) Present a description of some of the mechano-electrochemical events which occur in cartilage explants during loading.

Design: A thorough and provocative discussion on the effects of loading on articular cartilage will be presented. Five simplest loading cases are considered: hydrostatic pressure, osmotic pressure, permeation (pressure loading), confined compression and unconfined compression. Details of how such surface loadings are converted or transduced by the extracellular matrix (ECM) to pressure, fluid, solute and ion flows, deformation and electrical fields are discussed.

Results: Similarities and differences in these quantities for the five types of loading are specifically noted. For example, it is noted that there is no practical mechanical loading condition that can be achieved in the laboratory to produce effects that are equal to the effects of osmotic pressure loading within the ECM. Some counter-intuitive effects from these loadings are also described. Further, the significance of flow-induced compression of the ECM is emphasized, since this frictional drag effect is likely to be one of the major effects of fluid flow through the porous-permeable ECM. Streaming potentials arising from the flow of ions past the fixed charges of the ECM are discussed in relation to the flow-induced compaction effect as well.

Conclusion: Understanding the differences among these explant loading cases is important; it will help to provide greater insights to the mechano-electrochemical events which mediate metabolic responses of chondrocytes in explant loading experiments.

Key words: Articular cartilage, Mechanical signal transducer, Explant loading experiment, Flow-induced compaction.

Introduction

Articular cartilage serves as the load-bearing material of diarthrodial joints, with excellent friction, lubrication and wear characteristics [1]. It also serves to absorb mechanical shocks and to distribute the joint loads more evenly across the underlying bony structures. From a biomechanical standpoint, these important functional characteristics rely on the multiphasic nature of articular cartilage [2–11]. Simply, the tissue is a nonlinearly permeable, viscoelastic material consisting of three principal phases: (1) a charged solid phase, which is composed predominately of a densely-woven, strong, collagen fibrillar network enmeshed with a high concentration of charged proteoglycan aggregates (about 20% by wet weight); (2) a fluid phase which is water (normally <80% by wet weight); and (3) an ion phase which has many ionic species of dissolved electrolytes (Na^+, Ca^{++}, Cl^-, etc; <1% by wet weight) that are required to neutralize the charges fixed to the solid matrix [3, 5, 10]. Together, the fluid phase, the ion phase and the relatively soft charged solid matrix yield a diversity of observed mechano-electrochemical (MEC) phenomena [5, 10]. These three phases provide a tissue that is quite remarkable in its ability to withstand enormous compressive loads (many times body weight), and the associated high compressive stresses, that are applied onto the tissue [12, 13]. In a recent publication, compressive stresses as high as 20 MPa in the hip have been reported (approximately 3000 pounds per square inch) [14]. The ability of the tissue to withstand such high compressive stresses (without being crushed) is due to the multiphasic nature of the articular cartilage, and the unique and specific combination of the related coefficients of the tissue (i.e., porosity, permeability, conductivity, diffusivity, elastic moduli, and their inhomogeneous and anisotropic distributions within the tissue) [2–5].

Address correspondence to: Dr Van C. Mow, Orthopaedic Research Laboratory, Department of Orthopaedic Surgery, 630 W 168 Street, Black Building, Room 1412, Columbia University, New York, NY 10032. Tel.: 212-305-1515; Fax: 212-305-2741; E-mail: vcm1@columbia.edu

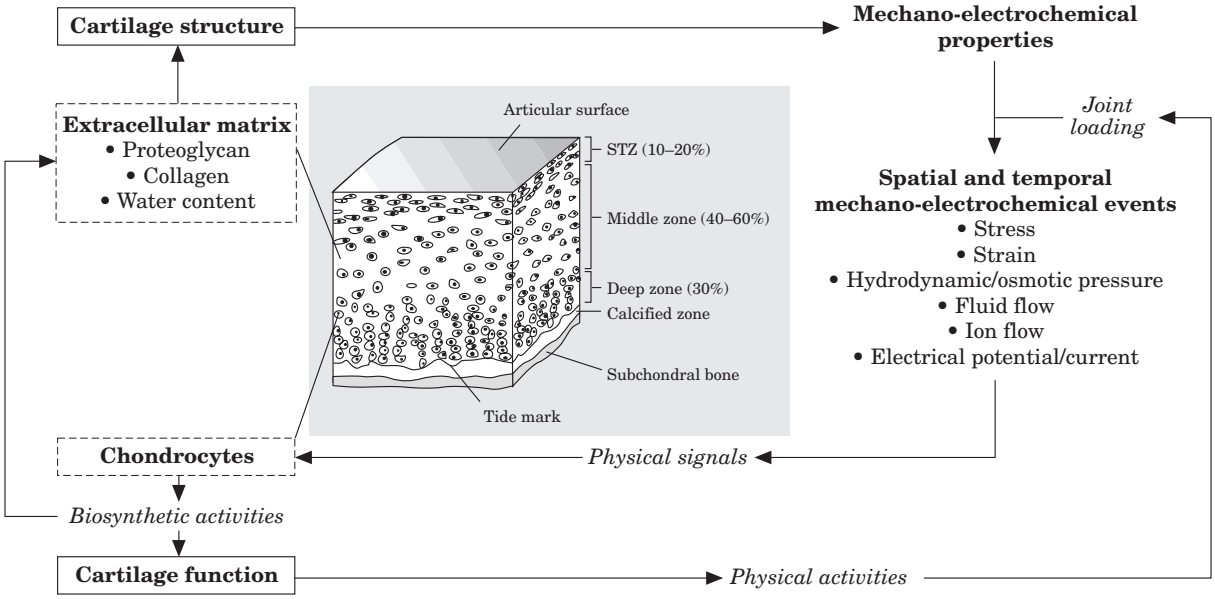

FIG. 1. Illustration of articular cartilage structure and chondrocyte distribution, and the inter-relationships between composition, MEC signals and chondrocyte biosynthetic activities.

Articular cartilage is a metabolically active tissue, and is synthesized and maintained by terminally differentiated chondrocytes that comprise less than 10% of the matrix by volume and/or weight [15–17]. The composition and organizational structure of the solid organic matrix, commonly referred to as the extracellular matrix (ECM), shields the ensconced chondrocytes from the high stresses and strains generated by joint loading, while not completely isolating the cells from their mechanical environment [18–21]. Analogous to the stylus of a phonograph, for example, the ECM, with associated interstitial fluid, solutes and ions, can collectively be thought of as a mechanical signal transducer that receives mechanical input in the form of joint or explant loading and yields an output of various extracellular signals (e.g., deformation, pressure, electrical, as well as fluid, solute (e.g., nutrient), and ion flow fields). These transduced signals in turn define the cell milieu *in situ* and may act independently or in combination to influence activities of the chondrocyte, or alternatively, be ignored by the chondrocyte.

The mechanism(s) by which chondrocytes convert physical stimuli to intracellular signals (e.g., mechanotransduction in the case of mechanical stimuli), which in turn direct cell activities, represent an area of intense orthopaedic research. An important step toward the identification of these mechanisms is a description of the exact nature of the chondrocyte MEC environment *in situ* (Fig. 1) [16–23]. In response to these issues, the biomechanical factors required to assess the MEC environment of the chondrocyte under five simplest, cartilage explant loading cases will be reviewed in this paper. It will become apparent, however, while some explant experiments adopted to study the biological response of cartilage to loading appear deceptively simple (e.g., immersing an explant into a bath of polyethylene glycol (PEG) solution for osmotic loading), these loadings produce unanticipated complex events within the ECM, thus leading to unwarranted interpretations of explant experimental data [22, 23].

From the bioengineering perspective, one challenge to defining the chondrocyte MEC environment is the development of detailed and accurate constitutive laws (i.e., a generalization of the simple stress–strain laws for common materials such as metals and plastics) for articular cartilage and chondrocytes (or any cell for that matter). For without these constitutive laws, it is not possible to calculate the deformational states within the ECM nor chondrocytes. Indeed, the entire area of constitutive modeling of articular cartilage's MEC behaviors [2–5] offers exciting new challenges for future bioengineering investigations.

Here is an illustration of the need for a detailed bioengineering analysis of cartilage during loading. It has been recently shown that the pressure produced in the interstitial fluid by PEG-osmotic loading of cartilage explant [23] is not equivalent to the pressure produced in any of the commonly used mechanically loaded explant experiments nor by hydrostatic loading [24], Fig. 2. This simple but often misunderstood PEG-osmotic loading result

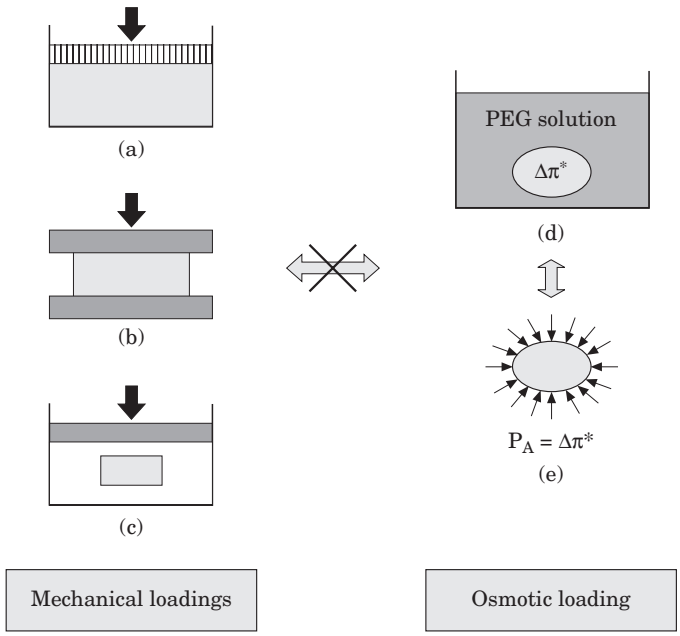

FIG. 2. Commonly used mechanical and osmotic loading explant experiments; (a) Confined compression with a rigid confining chamber and a rigid, permeable-porous loading platen (top); (b) Unconfined compression with two frictionless or frictional impermeable loading platens; (c) Hydrostatic pressure loading by pressurizing the bath solution; (d) Osmotic pressure loading using solutions with known osmotic pressure (e.g., polyethylene glycol solution of known concentration); (e) The 'equivalent' mechanical loading to the osmotic pressure loading in (d)—the mechanical load must be applied isotropically onto the explant with the applied load equal to the osmotic pressure applied in (d), and exactly normal to the surface.

clearly demonstrates the need for better theoretical models to analyze and to interpret biologic data from such osmotically or mechanically loaded explant experiments. As another example, numerous past studies have demonstrated that endothelial cells respond to viscous shear stresses in the flowing blood. Only recently has a bioengineering analysis been performed on the state of stress in endothelial cells and their cell membranes that actually provides a candidate mechanotransduction mechanism [25]. These authors concluded from their study that attention should be diverted from shear stress in the blood to the principal stresses in the cells, and how cell membrane stresses might be transmitted to the cell nucleus, thereby eliciting a response.

A major goal of this article, and of this special issue of *Osteoarthritis and Cartilage*, is to provide readers with an overall appreciation of the biomechanical factors that are required to analyze and interpret data from mechanically or osmotically loaded explant culture experiments.

Factors influencing mechano-electrochemical signals in the ECM of articular cartilage

What are the factors that might influence the MEC signals, i.e., the states of stress, strain, pressures (osmotic and hydrodynamic), and fluid and ion flows, that are transmitted through the ECM to the chondrocyte and its nucleus? Clearly, the manner of MEC signal transmission depends entirely on the nature of the transmitting medium (e.g., whether the material is an insulator or a conductor, or whether the material contains water and dissolved ions). One factor is therefore the ECM composition, particularly its spatial organization through the depth of the tissue and around chondrocytes. Another factor, and the simplest, is obviously the location of the cell within the tissue and its position relative to the external boundaries of the loaded explant in culture (Figs 1 and 2). The nature of the applied loading is also a factor. For example, is the explant loaded statically or dynamically; is the loading uniformly applied around the entire boundary or is the loading only along a portion of its boundary (Fig. 3)?

Functionally, the most important aspect of cartilage composition is its water content and fixed charge density [3–5, 10, 26–28]. Factors relating to the organization of the ECM macromolecules (e.g., various types of collagen and proteoglycans) [17, 29, 30], and of the heterogeneous cellular and compositional distributions within the tissue [10, 15, 17, 19, 31–36] also play significant roles in defining the MEC environment around chondrocytes [31, 36]. For example, the

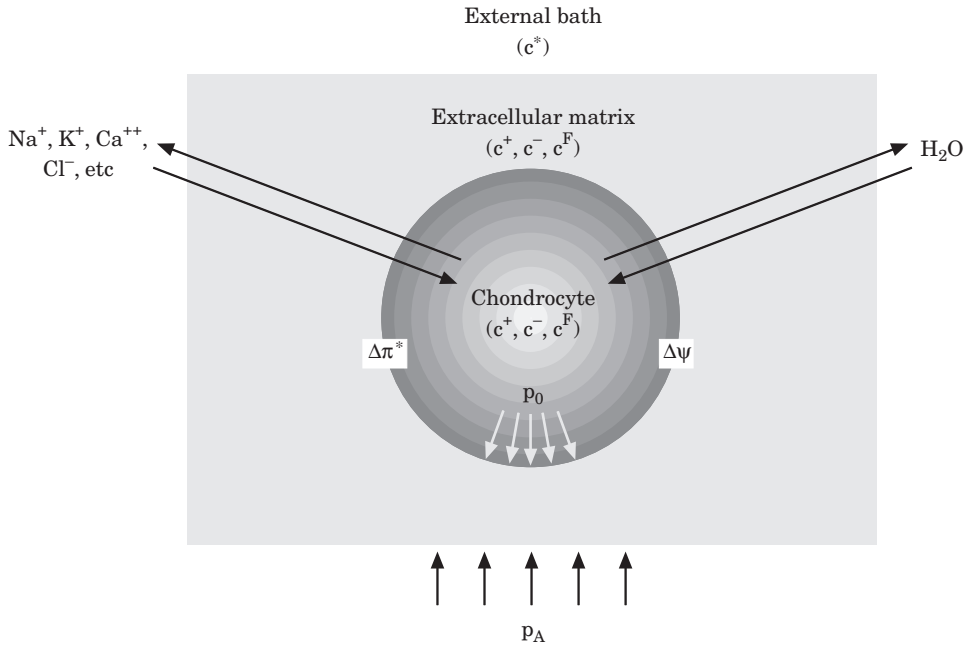

FIG. 3. Illustration of the MEC events experienced by chondrocytes and the interaction between ECM and chondrocytes; $\Delta\pi^*$ is the osmotic pressure jump and $\Delta\psi$ is the electrical potential jump across the cell membrane, respectively.

nature (e.g., tension, compression and shear) and magnitudes of the other MEC signals transmitted to the cells *in situ*, and thus to the nucleus, are all affected by the MEC properties of the ECM and that of pericellular matrix (PCM). In addition, and perhaps more fundamentally, it is not known to which stimuli these cells are responding (e.g., fluid pressure or solid stress, viscous shear stress or frictional drag force, osmotic pressure or hydrodynamic pressure)? Indeed, finding the answer to this question represents a major goal for many biologists and biochemists who have adopted explant loading in their research. There can be no specific answers, however, until a clear definition of the in-situ MEC environment surrounding the cells is available for well-designed and well-controlled explant loading experiments.

CHARGED NATURE OF ARTICULAR CARTILAGE

A major compositional factor, one that has received intense biochemical and physiochemical scrutiny over the past several decades, is the charged sulfate (SO_3^-) and carboxyl (COO^-) groups attached to the chondroitin sulfate chains, the sulfate group attached to the keratan sulfate chains, and the carboxyl group attached to the hyaluronan chains that comprise the major glycosaminoglycans (GAG) of the proteoglycan aggregate in cartilage [3, 5, 10, 20, 29, 30]. These charges are spaced between 10 and 15 angstroms apart along the GAG chains, and they give rise to a high charge density within the tissue (per unit interfibrillar solvent volume). This is commonly known in the literature as the 'fixed charge density' or simply FCD (measured in mEq/ml units; in normal articular cartilage the effective FCD ranges from 0.04–0.2 mEq/ml; [10]). These charges, or the effective FCD, produce profound effects not only on tissue hydration and control of fluid and ion transport through the interstitium [3, 5, 10, 27, 28], but also on a broad spectrum of other observed MEC responses such as streaming potentials. All of these MEC effects due to the effective FCD may be important in eliciting chondrocyte responses *in situ*. Only recently has the bioengineering literature advanced sufficiently to provide a clear understanding of these important MEC phenomena within the tissue [3, 5, 27, 28].

DONNAN OSMOTIC PRESSURE

To many orthopaedic, OA and cartilage researchers, the use of Donnan osmotic pressure to describe cartilage swelling has been an enigma. It is perhaps simplest to consider an elemental volume (as in differential calculus) of articular cartilage containing typical amounts of collagen, proteoglycans (i.e., charges), water, ions, cells, etc. At this micro-scale, this elemental volume acts like a microscopic osmotic chamber. The semipermeable membrane of the osmotic chamber is

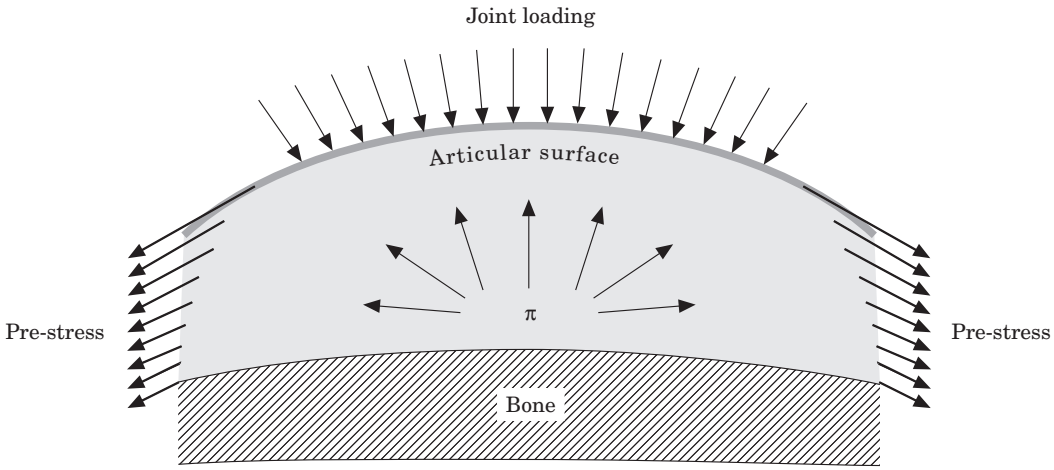

FIG. 4. Illustration of ECM pre-stress and osmotic pressure inside articular cartilage that is subjected to applied loading at the articular surface.

analogous to the strong, collagen network that surrounds and traps the large negatively-charged proteoglycans within the tissue. When the semi-permeable membrane of this micro-osmotic chamber is placed against an external electrolyte solution (e.g., NaCl solution at any concentration), water and ions will flow into (and out-of) the micro-osmotic chamber so as to maintain electroneutrality and to achieve electrochemical equilibrium with the charged proteoglycans contained within the micro-osmotic chamber [3, 5, 37–39]. In 1924, FG Donnan derived a mathematical expression for the equilibrium ion concentration (e.g., Na^+) within such a semi-permeable chamber of charged macromolecules [39]. The equilibrium ion concentration (c) for an idealized solution is given by the following simple quadratic formula:

$$c(c+c^F)=(c^*)^2, \tag{1}$$

where c^F is the FCD within the tissue, and c* is the ion concentration in the external bathing solution. Thus if the fixed charged density c^F is known (e.g., measured by some biochemical method [10]) and external ion concentration c* is given, then the ion concentration c inside the tissue can be easily calculated. The extra ion concentration (due to the need to maintain electroneutrality against c^F, which attracts counter ions such as Na^+) causes an imbalance of the freely mobile ions between those within the semi-permeable chamber (in the interstitium of the tissue) and those in the external bathing solution. The colligative effect of this imbalance creates an osmotic swelling pressure whose magnitude is determined by the concentration difference across the semi-permeable membrane, and may be calculated by using the simple van't Hoff pressure law [40]:

$$\Pi=RT[\varphi(2c+c^F)-2\varphi^*c^*]. \tag{2}$$

Here, R is the universal gas constant, T the absolute temperature, φ and φ* are the osmotic coefficients of the ions within the tissue and the external bathing solution, respectively. This expression defines the famous Donnan osmotic pressure of polyelectrolyte solutions. Over the past three decades, this expression has been adopted by some researchers to define the swelling pressures in articular cartilage [10, 23, 41, 42]. Recently, this expression for the swelling pressure has been derived using a multiphasic continuum approach [5], and a micro-structural modeling approach [43]. In the micro-structural approach, the repulsive force between two glycosaminoglycan chains (modeled as two rigid charged rods with charged density c^F), immersed in an electrolyte solution of concentration c*, was calculated and shown to yield equation (2) [43].

RESIDUAL STRESS IN ARTICULAR CARTILAGE

When a tissue is equilibrated in an external bathing solution containing dissolved electrolytes, a state of mechanical stress must exist within the solid matrix to balance this Donnan osmotic pressure [41, 44–47]. This equilibrium stress state within the ECM is known as a 'residual stress or pre-stress' (Fig. 4). In many engineering structures (e.g., pre-stressed reinforced concrete), a state of residual stress or pre-stress is deliberately created to enhance their load carrying capacity. In biologic tissues, these naturally occurring states of

residual stress have also been hypothesized to enhance the ability of various biologic tissues, in particular cartilage, to bear load [44–47]. Such states of pre-stress may be readily visualized when a small piece of cartilage is excised from the bone and equilibrated in a hypotonic solution. In this situation, the sample will always curl with the surface zone (the dense collagen rich zone) facing toward, and the deep zone (the proteoglycan rich zone) facing away from the center of curvature, respectively [46, 47]. Since residual stresses profoundly affect the states of stress acting within any material, they will therefore also profoundly affect the states of stress in the ECM and hence the states of stress seen by chondrocytes *in situ*. Also, since articular cartilage, and therefore chondrocytes, exist largely in an isolated physiologic environment [15], then it would seem that to understand how MEC signals are transmitted through the ECM to chondrocytes *in vivo*, or in explant experiments *in vitro* (Figs 2, 3) one would have to know some basic bioengineering concepts related to charged-hydrated soft tissues [2–5].

Objective

This article is aimed at introducing the reader (especially colleagues from the biological sciences interested in articular cartilage research) to some current and important concepts regarding the biomechanics of articular cartilage. It will address the following topics: (1) how cartilage deforms and supports load; (2) how fluid pressures are developed in the interstitium; (3) how electrical potentials and currents are generated within the tissue; (4) how these various MEC events might vary from location to location within the tissue; and (5) how these phenomena are intrinsically coupled. Clearly, this knowledge is necessary for the eventual unraveling of the mysteries surrounding the mechanical signal transduction mechanisms between the ECM, PCM and chondrocytes.

While animal models have made major gains in understanding cartilage pathophysiology following joint injury or altered joint function *in vivo*, e.g., joint immobilization or altered loading [48–51], these in-vivo studies do not provide an opportunity for determining the exact nature of the altered states of stress and strain, and other important MEC states, *within* the tissue. Thus, it is impossible to identify the specific mechanism(s) responsible for changes to the articular cartilage in these animal models. In other words, all these studies lack specificity in terms of cause-and-effect. Indeed, just what are the MEC signals that are important in altering chondrocyte metabolism? In an attempt to obtain specificity regarding MEC signal transmission, many investigators have turned to more simple loading configurations in their in-vitro explant experiments, with the hope of isolating the specific MEC signal(s), [Fig. 2(a)–(d)], that might have stimulated the observed changes in chondrocyte activities [16–23, 35, 36]. As will be seen below, despite even these simple loading experiments, analyses of the MEC events are more complicated than suspected.

From the engineering view point, this situation necessitates an appropriate constitutive law to determine: (1) how the MEC events vary spatially within the ECM; (2) the temporal nature of the MEC events; (3) the MEC events which dominate at each cell location within the tissue, and when. There are few loading conditions that produce a pure MEC signal, though they are of limited physiologic relevance. For most explant studies reported in the literature, however, a clear interpretation of biologic data has been confounded by the presence of many complex, intrinsically coupled MEC events. [22, 23, 52–55]. Therefore, the second major objective of this paper is to provide a description of some of the MEC events occurring within articular cartilage explants during a loaded in-vitro experiment, addressing the three questions enumerated above.

Explant loading experiments

As mentioned above, in-vivo studies of MEC events within articular cartilage are limited by the inability to precisely control the magnitude and distribution of the loading that articular cartilage experiences *in vivo*. However, given a stable and controlled biochemical and physical environment, cartilage explants can be maintained *in vitro* for relatively long periods of time, permitting study of their metabolic activities. Such explant cultures of cartilage can preserve the chondrocyte biosynthetic phenotype, as well as the potentially important interactions between the ECM and the cells. Also, in carefully crafted in-vitro experiments, it is possible to create and calculate (with the help of mathematical models) all the MEC signals within the cartilage explant. This obviously will be necessary for a better understanding of how signals are transmitted through the ECM to the chondrocytes. There are many ways to load an explant [e.g., Fig. 2(a)–(d)], and indeed many of these studies have been performed. In the sections below, we present short descriptions of what happens within the tissue in some of the loaded explant culture studies.

HYDROSTATIC PRESSURE

It has been shown that the high loads transmitted across joints during weight bearing are predominantly supported via the hydrostatic pressure developed within the interstitial fluid of articular cartilage [1, 56, 57]. The important components of the articular cartilage, i.e., the solid phase and the fluid phase, have been shown to be effectively incompressible [2, 58]. As a direct consequence of this result, a state of zero deformation and zero strain will exist throughout the ECM, even at high pressures. However, the state of stress and pressure in the tissue is non-zero. These quantities are isotropic and uniformly distributed throughout the ECM, whether or not the ECM internal structure is inhomogeneous or anisotropic. This applied hydrostatic pressure will always be supported by both solid and fluid phases, directly proportional to the porosity (φ^f=volume of fluid/total volume) and solidity (φ^s=volume of solid/total volume) at each point within the tissue (note these volume fractions must satisfy the following simple equation $\varphi^f+\varphi^s=1$; note also that the volume fraction of ions φ^i in solution is much less than 1). In other words, if the solidity φ^s is 20%, and the applied hydrostatic pressure is 5.0 MPa, then the hydrostatic pressure applied onto the ECM is only 1.0 MPa. Moreover, the surface traction applied at the chondrocyte boundary must also be isotropic, i.e., they must always act normal to the cell membrane (Fig. 3). This loading configuration can be achieved by simply pressurizing the fluid bath surrounding the tissue [Fig. 2(c)].

Hydrostatic pressure has been known to induce changes in chondrocyte metabolic activities. While intermediate levels (2.6–5 MPa) have been shown to increase the synthesis of proteoglycan and RNA [59, 60], lower pressure levels (0.35–2.1 MPa) have been found to decrease, or produce no change, in biosynthetic activities of chondrocytes [59–61]. When subjected to static non-physiologically high levels of hydrostatic pressure (20 or 50 MPa), proteoglycan synthesis has been observed to decrease, and this decrease was irreversible after the removal of the pressure [22]. In this study, it was also found that proteoglycan synthesis was elevated under short durations of high pressure loading (20s). For an excellent review of hydrostatic loading of cartilage explants, see reference [16].

OSMOTIC PRESSURE

Another simple test is an osmotic loading explant study. In these studies, the osmotic loading is applied onto the tissue by immersing it in a solution of known osmotic pressure, typically a solution of PEG [Fig. 2(d)]. Using this loading, the volume (or water content) of the tissue will decrease and therefore produce an effect which is similar to, but not the same as that of a mechanically applied compressive loading [Fig. 2(a)–(d)] [24, 42, 62]. The proteoglycan synthetic activity has been found to be reduced by such a hydrostatic pressure or osmotic pressure loading [23].

In some studies, the osmotic pressure loading using PEG solutions has been assumed to be equivalent to a mechanical loading whose magnitude is the same as the magnitude of the osmotic pressure [23, 42]. However, using the recently developed triphasic theory [3], a mathematical analysis has been performed to determine the conditions of this equivalence. It was found that the equivalence of osmotic loading and mechanical loading on cartilage (or any charged-hydrated tissue) is highly restrictive, i.e., they are equivalent, in terms of matrix deformation, only when the tissue is mechanically loaded in an isotropic and uniform manner [24], with the applied load equal in magnitude to that of the osmotic pressure. Even in this very restricted case, the interstitial pressures acting on chondrocytes *in situ* are not equivalent. In practice, therefore, there exists no equivalent mechanical load to the osmotic load [see Fig. 2(a)–(d)]. Thus, for studies wishing to address the effects of interstitial pressure on chondrocyte metabolism, it is critical to realize that the interstitial pressure within explants under mechanical loading is different than that generated by osmotic pressure loading. This result will profoundly affect the interpretations of tissue swelling in all previous hydrostatic and osmotically loaded explant experiments [10, 23, 42, 62]. Finally, it should be noted that while studies using osmotic pressure to load cartilage, in and of themselves, are not inappropriate, it is the interpretation of what the osmotic loading is doing in the explant *in situ* which needs to be re-examined.

These two loading experiments, hydrostatic pressure loading and osmotic pressure loading, are the two simplest possible tests that can be performed. In the hydrostatic pressure case, by virtue of the incompressibility of the solid and fluid phases [2, 58], when the tissue is immersed in the pressurized fluid bath, there is no motion, no deformation and no interstitial fluid flow. The pressure acting on the solid phase and the fluid phase is given by the applied hydrostatic pressure multiplied by the solidity φ^s and porosity φ^f,

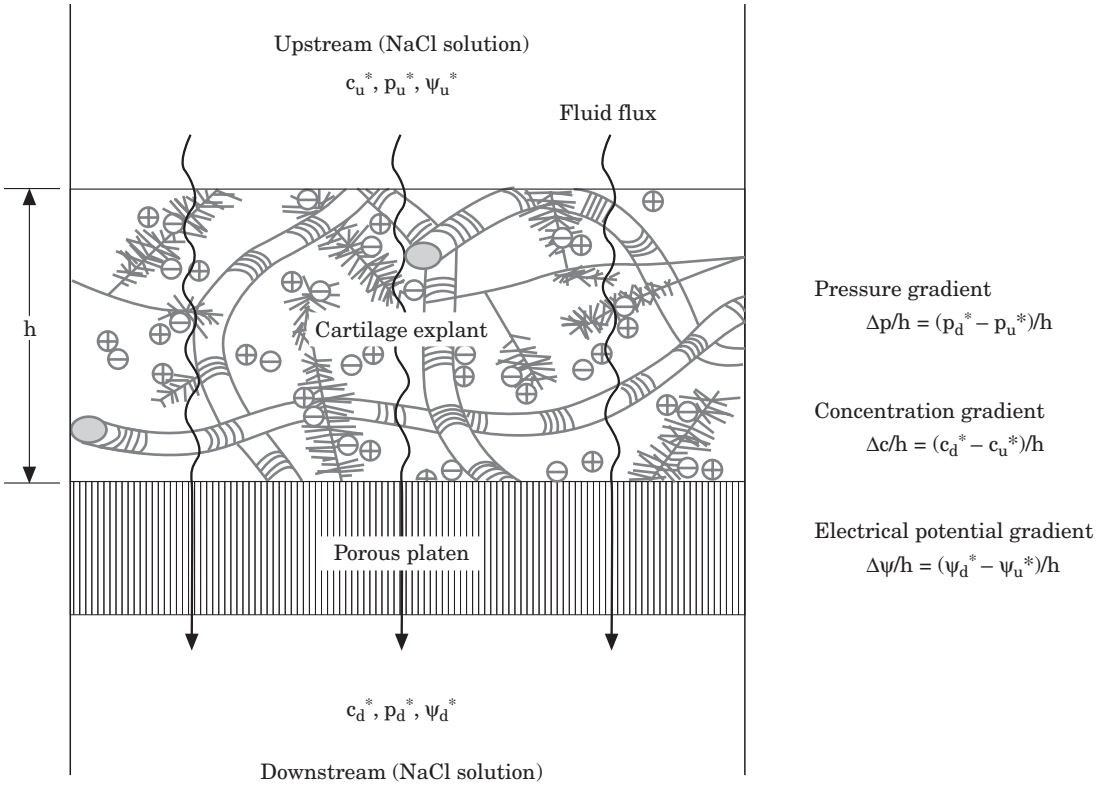

FIG. 5. Illustration of the one-dimensional permeation experiment; (c_u* and c_d*) are the NaCl concentrations upstream and downstream respectively; similarly (p_u* and p_d*) and (ψ_u* and ψ_d*) are the fluid pressures and electrical potentials respectively. The difference (Δ) of each quantity (i.e., the motive force) will cause fluid flow, ion transport and streaming potentials.

respectively. Under osmotic loading, there is deformation and interstitial fluid flow and loss. Moreover, the interstitial pressure generated by osmotic loading is equal to that generated by mechanical loading minus the osmotic pressure [24].

PERMEATION

The permeation test is the next simplest test, at least conceptually [5, 7, 10, 27, 28, 63–66]. At high pressures and strains (as is the case in the joint), this test is extremely difficult to perform and complicated to analyze [65, 66]. Today, this test is popular because of a number of tissue engineering applications in the biotech industry, where cartilage explants or chondrocyte seeded gels are perfused with a culture media to grow tissues for surgical replacements. To optimize the performance of such bioreactors, however, a thorough understanding of the mechanics of the permeation test [5, 27, 28, 66] is required. Because of the intrinsic coupling of MEC events within the ECM, understanding of how fluid flows through an explant or chondrocyte seeded gel in this experiment needs careful analysis as well.

To simplify the mathematical analysis, historically, all permeation (flow) experiments reported in the literature have been restricted to the one-dimensional (1D) case. Figure 5 is an illustration of such a 1D permeation experiment. For tissue such as articular cartilage (a soft, charged, hydrated, porous-permeable solid material), there are three types of motive forces that can drive fluid or ions through the specimen [5, 27, 28, 37, 38]: (1) a hydrostatic pressure gradient; (2) a concentration gradient; and (3) an electrical potential gradient. In the experiment, the cartilage explant of thickness h is placed upon a supporting porous-permeable platen, while a fluid containing a NaCl concentration is loaded above and below the sample. By imposing either a hydrostatic pressure gradient (p_d*–p_u*)/h, a concentration gradient (c_d*–c_u*)/h, or an electrical potential gradient (ψ_d*–ψ_u*)/h, or any combination of these driving forces, fluid and ions will flow across the tissue. For simplicity, we shall only consider the case of a hydrostatic pressure gradient. For a complete description of all three phenomena, the reader is referred to [5, 27, 28, 37, 38].

Recall that normal articular cartilage contains approximately 75% water by wet weight [7–11, 26].

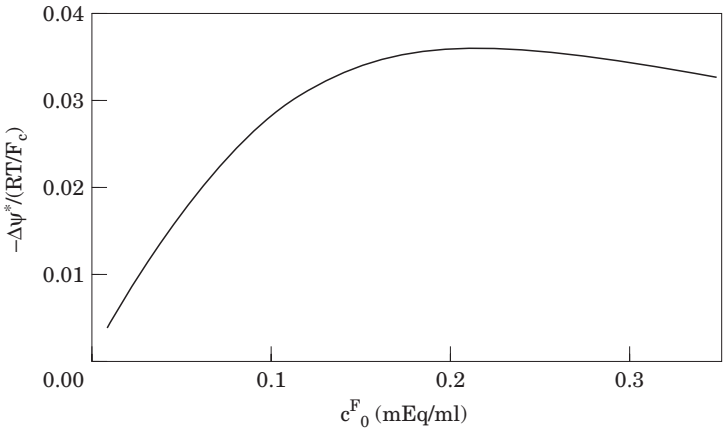

FIG. 6. Effect of cartilage fixed charge density (FCD) on the electrical potential difference between the external upstream and downstream solutions in a one-dimensional permeation experiment. The applied hydrostatic pressure difference is 0.05 MPa; RT/F_c is approximately 25.7 mV.

This water contains many dissolved electrolytes, but mostly NaCl [6]. For simplicity, it may be assumed that the total electrolyte concentration (c) in the interstitium is defined by the Donnan equilibrium ion distribution law, equation (1). While the charges on the proteoglycans do not flow with the interstitial fluid, i.e., they are fixed on the solid matrix, the dissolved electrolytes will be convected with the flowing interstitial fluid. Because of this asymmetry, when a hydrostatic pressure gradient is applied across the specimen (Fig. 5), the NaCl dissolved in the solution at the upstream side and within the tissue will be forced to flow through the specimen to the downstream side. It is important to note that the electrolyte concentration c within the tissue is always greater than c_u^* and c_d^* outside the tissue. So, as the fluid flows through the specimen, and in order to maintain electroneutrality within the specimen, an electrical potential (assuming zero current condition is imposed) must be established against the direction of water flow to restrict a loss of counterions (e.g., Na^+) from the tissue. Under these conditions, the streaming potential ψ is given by the following equation:

$$\Delta\psi = -c^F F_c k \Delta p/\kappa_o, \qquad (3)$$

see reference [27]. Here $\Delta\psi$ is the electrical potential across the specimen, F_c the Faraday constant, k is the permeability of the tissue and κ_o is the electrical conductivity of the tissue. Note that this equation explicitly defines the relationship between the FCD and the streaming potential (this point will be discussed later in this paper). In other words without the existence of the FCD in the ECM, there can be no streaming potential for articular cartilage. Figure 6 shows how this streaming potential will vary with the FCD at $\Delta p = 0.05$ MPa. It is of interest to note that the streaming potential reaches a maximum at exactly the physiologic range of FCD. This may have important physiologic implications. This simple example is an illustration of coupling between a mechanical phenomenon, i.e., fluid flow, and an electrical phenomenon, i.e., the streaming potential. Streaming potentials and currents are always generated when there is fluid flow (with ions) over a charged surface (under an open circuit condition), and must be considered in any interpretation of data from experiments that perfuse fluids across a cartilage explant, such as those used in bioreactor applications. For readers interested the closed circuit condition, see reference 27.

Another intrinsic coupling effect relates to the deformation of the ECM and interstitial flow through it. This mechanical-to-mechanical coupling between a solid and a fluid has been known for more than two decades [65, 66]. In subsequent years, it has been determined, experimentally and theoretically, that this coupling effect profoundly affects all load and deformational behaviors of articular cartilage [1, 2, 4, 26, 65–68]. Simply, as the hydrostatic pressure gradient drives the fluid relentlessly through the porous-permeable ECM, the fluid particles are forced to move through a torturous pattern of interconnecting pores and interstices in the collagen-proteoglycan solid matrix. The average 'diameter' of these pores has been estimated to be 60 angstroms in uncompressed tissues, and 30 angstroms in highly compressed tissues [10, 26]. Since the average flow speed through the tissues is around 1 micron/sec at 1 MPa, or 10,000 angstroms/sec, the average water molecule, 14 angstroms in diameter, will be flowing

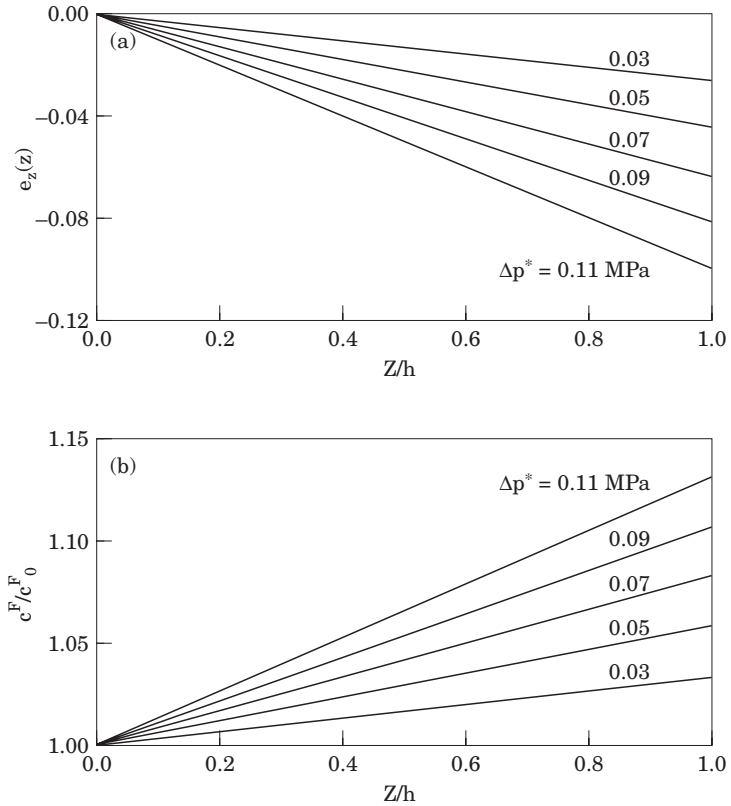

FIG. 7. Distributions of flow-induced compaction (**a**) and FCD (**b**) within the tissue under various applied pressure differences (Δp^*) in a one-dimensional permeation experiment. Before compression, the initial FCD (c^F_0) is 0.2 mEq/ml.

very fast indeed relative to the size of the pores in cartilage. As these water molecules negotiate their way through the pores and interstices, they must collide against the collagen and proteoglycan molecules of the ECM, causing an exchange of momentum and frictional dissipation [2, 4]. This frictional dissipation may be 1000 to 100,000 times greater than the viscous dissipation in the fluid. Because of this resistance to flow, the permeability of cartilage is very low (10^{-15} $m^4/N \cdot s$ units; a decimal point followed by 15 zeros—a very small number indeed).

Now, as the water flows from the high pressure upstream side to the low pressure downstream side, its energy is consumed in compacting the ECM (and to a lesser degree by frictional heating). This effect is known as flow-induced compaction of the ECM [66–68]. Figure 7(a) shows the compaction of the ECM caused by the flowing water molecules at various pressure gradients, for a FCD of 0.2 mEq/ml. This compaction increases from the upstream side (zero) to a maximum at the supporting porous-permeable platen at the downstream side. Figure 7(b) shows how this compaction effect influences the FCD through the depth of the tissue at various pressure gradients. Starting with an initial fixed charge density c^F_0=0.2 mEq/ml, for example, at a pressure difference of 0.11 MPa, the FCD can increase by 10% at the downstream side. (Undoubtedly, this change in FCD will also affect the streaming potential effect discussed above.) Since both ECM compression and FCD can affect chondrocyte metabolism [16, 69], it is therefore important to realize how these quantities change with location in the tissue.

It is clear that even in the simple 1D permeation experiment, many unanticipated effects occurring within the tissue can confound the interpretation of biologic data from explant experiments. These effects, derived from the intrinsic coupling of MEC phenomena, can only be understood with proper bioengineering modeling and analysis. Unfortunately, these coupled phenomena are usually nonlinear, thus making the analysis quite difficult. However, recent theoretical advances in these areas of investigation [2–5, 27, 28, 66–68] have opened doors to a new understanding of MEC signal transductions in articular cartilage.

CONFINED COMPRESSION

The previous three examples of loading of cartilage (hydrostatic pressure, osmotic pressure and hydrostatic-permeation) are achieved via an

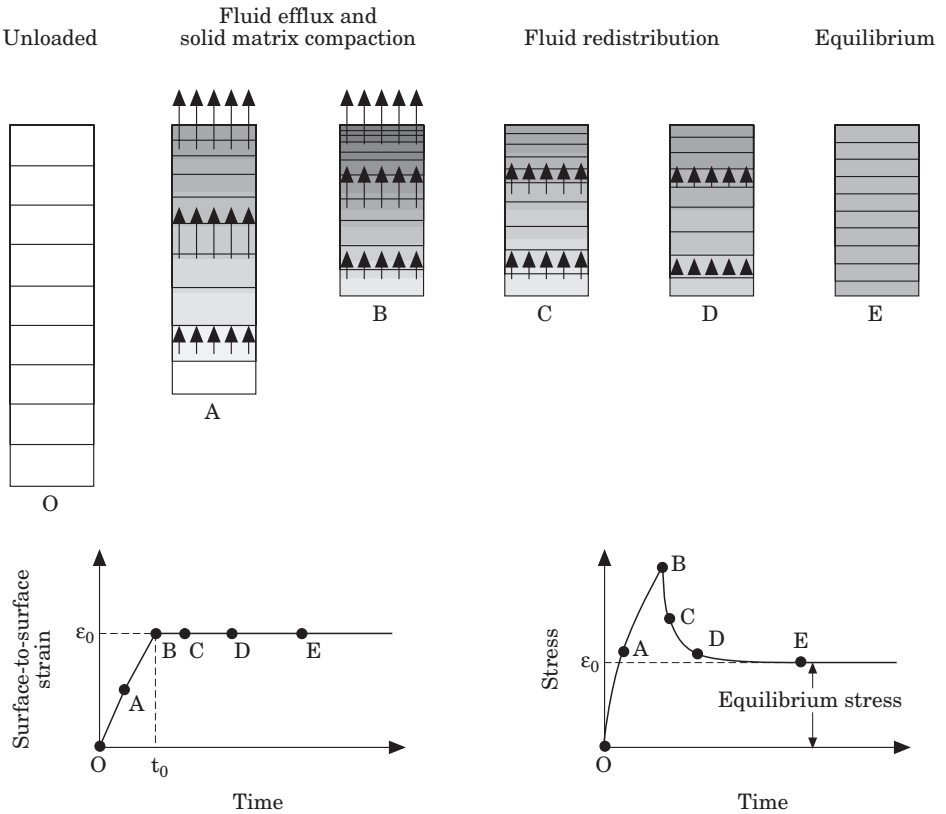

FIG. 8. Schematic representation of fluid exudation and redistribution within cartilage during a rate-controlled, confined compression, stress-relaxation experiment (**lower left**). The horizontal bars in the upper figures indicate the distribution of strain in the tissue over the duration of the experiment. The lower graph (**lower right**) shows the stress response during the compression phase (O,A,B) and the relaxation phase (B,C,D,E).

imposed fluid pressure loading. But for articular cartilage, other types of loading also occur *in vivo*. Mature articular cartilage is normally attached firmly to the impermeable subchondral bone, and articulates against an opposing articular surface [12–14, 70, 71]. Thus one needs to examine how articular cartilage will respond when pressed against a solid material, loaded either by a porous-permeable [2, 4, 67] or a frictionless-impermeable solid loading platen [75]. The first such study (the next simplest test described in this paper) to investigate is the 1D confined compression test [Fig. 2(a)] [2, 4, 11, 67]. In this problem, everything (deformation and fluid flow) moves axially, i.e., in the direction of the applied load [Fig. 2(a)]. This test requires a precisely prepared cylindrical plug of cartilage removed from a joint surface. The experiment calls for inserting this cartilage specimen into a frictionless, impermeable confining chamber (to prevent lateral expansion and fluid flow), with the articular surface axially loaded against a rigid-porous-permeable solid loading platen [Fig. 2(a); top] and the deep zone loaded against a rigid impervious surface [Fig. 2(a); bottom]. The top rigid porous-permeable platen permits the interstitial fluid to flow into the pores of the platen, as it exudes from the tissue. The pore pressure within this loading platen is ambient, so the exudation can flow freely into the pores of the loading platen (without any back pressure). The bottom rigid impervious platen simulates the attached bone; there is no fluid exudation at this surface.

In a loading experiment such as the one described, one needs to be specific as to what is really being imposed: (1) a compression (say 10% strain); or (2) a load (say 1 MPa). The first type of loading defines a stress–relaxation experiment, while the second type of loading defines a creep experiment. In this section, only the stress-relaxation test will be described, Fig. 8 [2, 4, 67]. The reader may refer to these references for a complete description of the biphasic confined-compression creep test as well. Understanding of this biphasic stress-relaxation process for articular cartilage is fundamental in understanding how the solid and fluid phases of cartilage contribute to its deformation behavior and ability to support load.

In as much as a deformation cannot be instantaneously imposed (this would violate Newton's 2nd law of motion), and in order to design a well-defined experiment, one can impose a deformation or displacement us defined by a ramp function having a given speed, $\varepsilon_o h/t_o$ (Fig. 8; bottom left). This means that the surface-to-surface strain ε_o (say 10%) is imposed, say in a linear manner, over the time duration $0<t<t_o$ (e.g. 200 seconds). For time $t>t_o$, the strain ε_o is maintained constant for the remainder of the experiment (say 10,000 seconds). The time history of the stress response (i.e., the stress required to impose the deformation defined by Fig. 8, bottom left) is given by Fig. 8, bottom right. Now, because the porous-permeable solid matrix is being forced back into the incompressible interstitial fluid at the prescribed speed of $\varepsilon_o h/t_o$, and because the permeability is very low, a large resistance will be generated. Note that as the surface-to-surface compression increases from O–A–B, the stress response rises to a maximum at B (above the equilibrium level σ_f). For $t>t_o$, the stress-relaxation phase, the stress required to maintain the strain ε_o will relax from the peak value at B to some equilibrium stress σ_f. This stress-relaxation process is caused by fluid redistribution within the tissue, see Fig. 8 (top boxes).

The boxes in Fig. 8 (top) show how the compressive strain and interstitial fluid flow occur within the tissue during the compression phase ($0<t<t_o$; boxes O, A and B) and the relaxation phase ($t>t_o$; boxes B, C, D, E) of the stress-relaxation experiment. At time $t=0$, there is no compression of the tissue, as illustrated by the large grid spacing in the diagram (box O). During the compression phase (O–A–B; $0<t<t_o$), fluid exudation occurs and the rate of exudation is constant. This is a consequence of the incompressibility condition, where compression of the tissue can only occur when there is fluid exudation (boxes A and B). Also, during the compression phase, matrix compaction is confined to the top regions of the tissue, as illustrated by the fine grid spacing (boxes A and B). During the relaxation phase, because no additional compression takes place, no exudation will further occur. Stress relaxation occurs due to the relief of the high compressive strain at the top regions of the tissue causing an internal re-distribution of the interstitial fluid (boxes C and D). At equilibrium ($t\rightarrow\infty$), no fluid flow occurs, and all transients die out (box E). The equilibrium stress σ_f defines the intrinsic compressive modulus (σ_f/ε_o) of the tissue.

An important point to note is that the surface-to-surface strain (ε_o) only represents the actual strain within the tissue as $t\rightarrow\infty$ (see Fig. 8, box E). For all other times, the actual strain within the tissue varies with depth, and can be much greater than ε_o at the porous-permeable loading platen—see boxes A, B, C, D. The value of the actual strain depends largely on the rate of compression ε_o/t_o; it is always the greatest at the porous-permeable loading platen. The use of ε_o as the sole parameter to describe compressive strains in tissue explants is obviously an oversimplification and represents the most common error in the field. From this example, it can be seen that by simply 'compressing' the tissue, many phenomena (potential cell stimuli) are occurring within the tissue or the loaded explant. However, as evident in the above paragraph, to the unsuspecting researcher interested in understanding how physical stimuli affect chondrocytes in articular cartilage, but unaware of these bioengineering complexities, it is fully understandable that incorrect interpretations may result.

In addition, one can inquire whether it is the compressive strain or interstitial fluid flow (with all its mechano–electrochemical phenomena) that have produced these biosynthetic changes. Recent short-term loading studies have demonstrated that transient fluid flow can affect chondrocyte proteoglycan metabolism [55, 72, 73], in contradistinction to earlier interpretations of data from similar experiments [52, 53], thus changing previous paradigms on matrix compression effects of chondrocyte metabolism. It is of interest to note the disparity between the interstitial fluid pressure at the impermeable interface, and at the porous-permeable interface (Fig. 9). At the impermeable interface (Fig. 2(a) bottom), almost all of the total applied stress is supported by the fluid pressure while at the porous-permeable interface, less than 50% is supported by the fluid pressure [56, 57, 74]. Thus, in any cartilage explant experiment that utilizes the confined compression test, it is critical to realize where the chondrocytes reside (Fig. 1), particularly with reference to the fluid pressure, compression and flow fields. Clearly, the homogenization of explants from such studies for biochemical measures, without regard for the chondrocyte MEC environment at different locales, can lead to misinterpretations. Finally, Fig. 10 shows another added benefit of FCD in articular cartilage. The peak stress at the end of the compression phase (Fig. 8; box B and Fig. 9; p_B) has been shown to depend on the FCD. Here it is seen that P_B increases many fold with increasing FCD, acting to provide a more effective load support mechanism for articular cartilage [74].

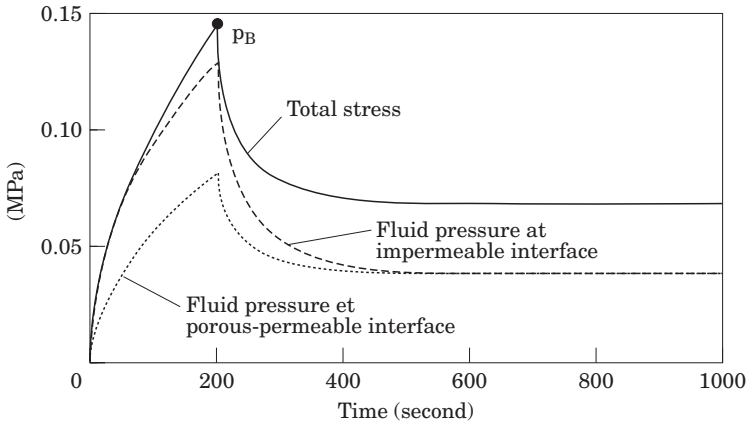

FIG. 9. The total stress and fluid pressure in a confined compression, stress-relaxation experiment. At the impermeable surfaces, nearly the entire total stress is supported by the fluid pressure. In contrast, at the permeable surface, only a small fraction of the total stress is supported by the fluid, with the remainder borne by the solid matrix.

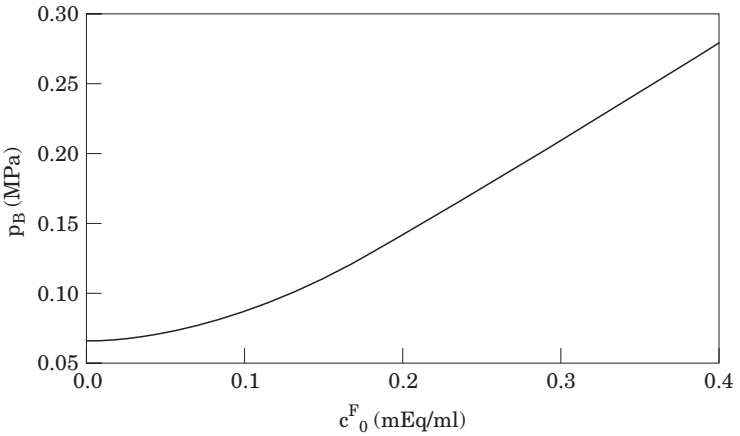

FIG. 10. Effect of initial fixed charge density (FCD) on peak stress (p_B) in a confined compression, stress-relaxation experiment. This result illustrates another beneficial contribution of FCD to the biomechanical function of articular cartilage.

UNCONFINED COMPRESSION

The confined compression analysis just described provides an easy and intuitive understanding of how matrix compression, fluid pressurization and flow, and strain generated streaming potentials will develop *in situ* when articular cartilage is compressed in the stress-relaxation mode. However, the confined compression explant experiment is difficult to achieve because of two technical difficulties: (1) it's not possible to achieve perfect confinement as the mathematical solution requires; and (2) the confining chamber prevents nutrients from accessing the articular cartilage. For these reasons, most compression explant studies have been performed using an *unconfined* compression test [18, 52, 53, 55, 73]. Similarly, both stress–relaxation and creep experiments can be performed in unconfined compression tests. In the section, only the creep experiment will be described.

A schematic representation of an unconfined compression test is shown in Fig. 2(b). The loading platens (top and bottom) are usually considered to be impervious and frictionless. The lateral walls of the cylindrical specimens are not confined, thus allowing free access to the bathing solution (e.g., tissue culture medium). While this loading configuration appears to be similar to the confined compression case [Fig. 2(a)], the deformation and flow fields are entirely different [2, 75]. As shown in Fig. 2(b), when the explant is loaded in the axial direction, compression in the axial direction can only take place when there is lateral deformation. Moreover, by virtue of the 'idealized frictionless' condition imposed at the loading platens, the compressive strain in the axial direction does not vary

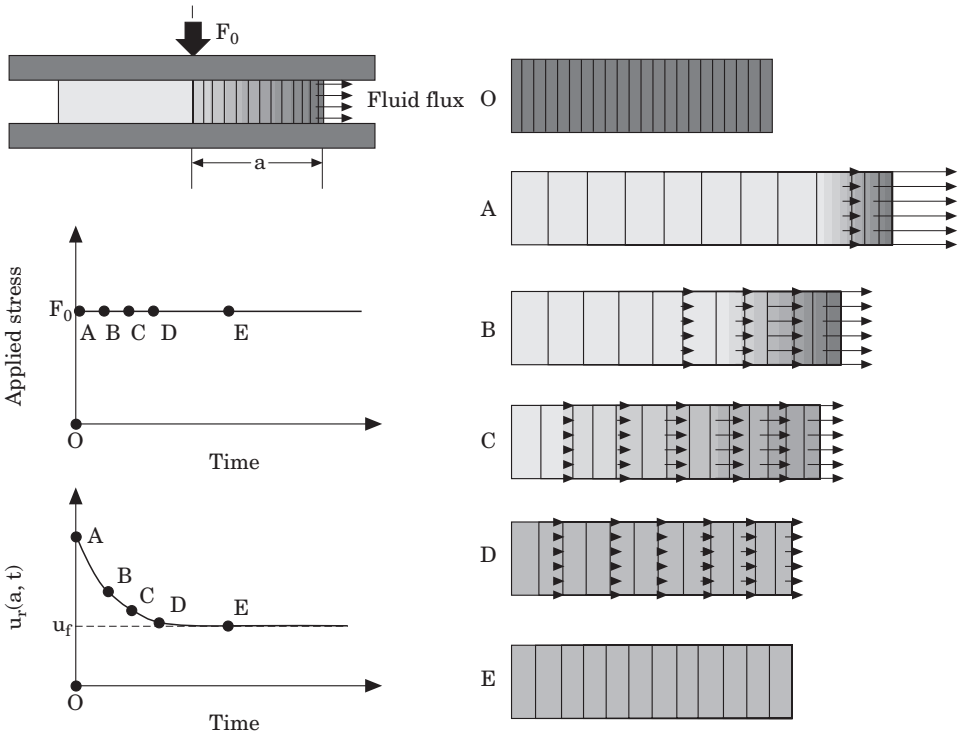

FIG. 11. Schematic representation of deformation and fluid flow within cartilage during a load-controlled (creep), unconfined compression experiment (**left top**). The bars within the right boxes indicate the distribution of radial strain in the tissue, and the arrows indicate the distribution and magnitude of flow rate. Since the tissue is in tension in the radial direction, the vertical grid indicates the radial distribution of tensile strain. The lower left graph shows the time history of the radial displacement at the edge of the specimen (r=a).

with depth through the tissue while the radial strain varies with the radial distance from the center of the explant as well as time [75]. During the initial loading period of this creep experiment, the change in volume of the solid matrix is maximal at the periphery which experiences the maximal fluid flow rate, Fig. 11. With increasing time afterwards, all fluid flow ceases, and the strain attains its equilibrium value. Interstitial fluid pressurization is maximal near the center of the specimen before equilibrium and eventually approaches the osmotic pressure defined by the Donnan osmotic law at equilibrium. Using the same nomenclatures adopted in Fig. 8 for the confined stress-relaxation experiment, Fig. 11 provides a summary of the deformation, radial strain and flow field within the explant at several time intervals (A, B, C, D, E) for the unconfined creep experiment. The important point to note is that in the unconfined compression test, while the strain in the axial direction [Fig. 2(b)] is always compressive, the strain in the *radial* direction is always tensile [Fig. 11 (as depicted by the grid width)]. Thus a chondrocyte at any location within the explant will be squashed in the axial direction and stretched in the radial direction. One therefore must ask, in view of the many cell stretching experiments reported in the literature (see article by Banes *et al* in this issue and [16]), to which mechanical signal (stretching or compression) have the chondrocytes responded to; or whether the chondrocytes have responded to the pressure, flow or electrical potential fields within the explant?

A number of advances have been made since 1984, when the first analysis of the unconfined compression problem appeared [75]. The case of frictional or adhesive loading platen was analyzed in 1990 to assess the frictional effects on the deformation and load support characteristics of the explant [76]. The inclusion of frictional stress at the loading platen dramatically altered the theoretical deformation, flow and pressure fields within the tissue; making them now vary with depth through the tissue. This variation of the flow and deformation fields in cartilage under unconfined conditions created perplexing difficulties in the interpretation of biologic results, see Fig. 11. To reconcile some of these differences, an unconfined compression study was pursued specifically to compare the spatial profile of MEC signals and spatial profile of biosynthesis [73]. In this 1995 study, the authors adopted the *ad hoc* electromechanical theory of [77, 78] that coupled fluid

flow and current density with hydrostatic fluid pressure and electric potential with the biphasic theory. In their unconfined compression explant test, and theoretical analysis, frictional-adhesive impermeable loading platens were used. In a subsequent study, the authors show that the calculated streaming potential and flow velocity, but not hydrostatic pressure fields were similar to their measured radial dependence of proteoglycan synthesis induced by dynamic unconfined compression [55].

While on the surface this analysis seemed to have included all the relevant parameters (matrix stresses and strain, hydrostatic pressure, fluid flow and electrical potential) [73], an in-depth examination of the electromechanical theory [77, 78] reveals that this theory does not include a description of the FCD nor ion movement in the tissue. Without an appropriate treatment of these fundamental characteristics of cartilage, one cannot attain a complete description of cartilage streaming potentials and streaming currents, nor can there be a Donnan osmotic pressure (see equations 1–3). In light of this fact, no answer is yet available on how MEC signals are transmitted through the ECM to the chondrocytes under the unconfined compression loading condition; a complete solution for the MEC signals in a confined compression analysis may be found in [74].

EXTENSION OF EXPLANT STUDY: VISCOUS SHEAR FLOW STUDIES OVER CELL CULTURE

As discussed above, fluid and ions can flow through the ECM. This flow is accompanied by an extremely high resistive force, which compacts the tissue in the direction of flow. This resistive force results from both a frictional resistance between the interstitial fluid and the porous-permeable ECM (i.e., a fluid–solid interaction) and a viscous shear stress within the interstitial fluid *per se*. It has been shown, however, that the frictional drag of fluid-solid interaction can range from 1000–100,000 times greater than the viscous drag in the fluid [79]. As a consequence, there is a significant compressive strain field within the tissue from the drag-induced compression effect [27, 66–68]; thus chondrocytes residing within the ECM will be similarly compressed [16, 35, 36]. By contrast, because of the low viscosity and shear rates within the tissue, the viscous shear effect would be minimal *in situ*. In recent times, a number of investigators have pursued viscous shear flow-induced changes in chondrocyte morphology and metabolism [80, 81]. While these studies are in and of themselves of scientific interest, all evidence of fluid flow within the interstitium of normal articular cartilage does not support the hypothesis underlying such studies that significant fluid shear stress exists within the tissue. Fluid shear may perhaps have application in tissue engineering of cartilage. If fluid flow resistance through the tissue has any effect, it is likely by either streaming potential, flow-induced compaction of the ECM, or convection of solutes and nutrients to chondrocytes residing in this avascular tissue.

Discussion

Explant loading experiments have been in existence for a long time [16]. Such studies have almost always included detailed and meticulous measurements of tissue biochemistry, altered gene expression, etc. Unfortunately, the same cannot be said of efforts to analyze the mechano-electrochemical events that are created in the tissue when it is loaded. A case for considering the ECM, associated interstitial fluid, solute and ions, as a mechanical signal transducer in articular cartilage has been made. Indeed, it is clear that the ECM provides a protective milieu for the chondrocyte to exist in while also serving as a mechanical signal transducer, which mediates the presentation of stimuli to the chondrocytes by directing the transmission of surface joint or explant loads to the chondrocytes *in situ*.

In this paper, the simplest loading conditions have been described, with a focus on the presentation of unanticipated and perhaps counter-intuitive results. Deformational complexities associated with these simple explant loading studies have, ironically, confounded the understanding of possible cellular mechanotransduction mechanisms for which they were designed to elucidate. This situation should provide cogent motivations for closer and more in-depth collaborative efforts between engineers and scientists aimed at the design and performance of explant loading experiments which yield the greatest insights. If pure MEC signals can be produced within the ECM, or if analyses can be made of all deformational events within the tissue to assess dominant effects, then better explant loading experiments may be designed and valid interpretations made. Under these conditions, great progress can be made toward understanding of mechanism(s) which mediate physical effects on chondrocytes *in situ*.

Acknowledgments

This work was supported in part by a grant from the National Institutes of Health AR 41913.

References

1. Mow VC, Ateshian GA. Lubrication and wear of diarthrodial joints. In: Mow VC, Hayes WC, Eds. Basic Orthopaedic Biomechanics. Philadelphia, PA: Lippincott-Raven Publishers 1997:275–315.
2. Mow VC, Kuei SC, Lai WM, Armstrong CG. Biphasic creep and stress relaxation of articular cartilage in compression: theory and experiments. J Biomech Engng 1980;102:73–84.
3. Lai WM, Hou JS, Mow VC. A triphasic theory for the swelling and deformational behaviors of articular cartilage. J Biomech Engng 1991;113:245–58.
4. Ateshian GA, Warden WH, Kim JJ, Grelsamer RP, Mow VC. Finite deformation biphasic deformation biphasic material properties of bovine articular cartilage from confined compression experiments. J Biomechanics 1997;30:1157–64.
5. Gu WY, Lai WM, Mow VC. A mixture theory for charged-hydrated soft tissues containing multi-electrolytes: Passive transport and swelling behaviors. J Biomech Engng 1998;120:169–80.
6. Linn FC, Sokoloff L. Movement and composition of interstitial fluid of cartilage. Arthritis Rheum 1965;8:481–94.
7. Edwards J. Physical characteristics of articular cartilage. Proc Inst Mech Engng 1967;181-3J:16–24.
8. Mankin HJ, Thrasher AZ. Water content and binding in normal and osteoarthritic human cartilage. J Bone Jt Surg 1975;64A:76–9.
9. Lipshitz H, Etheredge R, Glimcher MJ. Changes in the hexosamine content and swelling ratio of articular cartilage as functions of depth from the surface. J Bone Jt Surg 1976;58A:1149–53.
10. Maroudas A. Physicochemical properties of articular cartilage. In: Freeman MAR, Ed. Adult Articular Cartilage. Kent, UK: Pitman Medical 1979:215–90.23.
11. Armstrong CG, Mow VC. Variations in the intrinsic mechanical properties of human articular cartilage with age degeneration and water content. J Bone Jt Surg 1982;64A:88–94.
12. Serig A, Arvikar RJ. The prediction of muscular load sharing and joint forces in the lower extremities during walking. J Biomechanics 1975;8:89–102.
13. Paul JP. Joint kinematics. In: Sokoloff L, Ed. The Joint and Synovial Fluid. New York: Academic Press 1980:139–76.
14. Hodge WA, Fijan RS, Carlson KL, Burgess RG, Harris WH, Mann RW. Contact pressures in the human hip joint measured in vivo. Proc Nat Acad Sci 1986;83:2879–83.
15. Stockwell R. Biology of Cartilage Cells. Cambridge University Press 1979:7–31.
16. Guilak F, Sah RL, Setton LA. Physical regulation of cartilage metabolism. In: Mow VC, Hayes WC, Eds. Basic Orthopaedic Biomechanics. Philadelphia, PA: Lippincott-Raven Pub 1997:179–207.
17. Ratcliffe A, Mow VC. Structure and function of articular cartilage. In: Comper WD, Ed. Extracellular Matrix. Melbourne, Australia: Harwood Academic Publishers 1996:234–302.
18. Guilak F, Meyer BC, Ratcliffe A, Mow VC. The effects of matrix compression on proteoglycan metabolism in articular cartilage explants. Osteoarthritis Cart 1994;2:91–101.20.
19. Grodzinsky AJ, Frank EH, Kim YJ, Buschmann MD. The role of specific macromolecules in cell-matrix interactions and in matrix function: Physicochemical and mechanical mediators of chondrocyte biosynthesis. In: Comper WD, Ed. Extracellular Matrix. Melbourne, Australia: Harwood Academic Publishers 1996:310–34.
20. Mow VC, Bachrach NM, Setton LA, Guilak F. Stress, strain, pressure, and flow fields in articular cartilage and chondrocytes. In: Mow VC et al. Eds. Cell Mechanics and Cellular Engineering. New York, NY: Springer-Verlag 1994:345–79.
21. Mow VC, Setton LA, Guilak F, Ratcliffe A. Mechanical factors in articular cartilage and their role in osteoarthritis. In: Kuettner KE, Goldberg VM, Eds. Osteoarthritic Disorders. Rosemont, IL: Am Acad Orthop Surg Pubs 1995:147–71.
22. Hall AC, Urban JPG, Gehl KA. The effect of hydrostatic pressure on matrix synthesis in articular cartilage. J Orthop Res 1991;9:1–10.
23. Schneiderman R, Keret D, Maroudas A. Effects of mechanical and osmotic pressure on the rate of glycosaminoglycan synthesis in the human adult femoral head cartilage: An in vitro study. J Orthop Res 1986;4:393–408.
24. Lai WM, Gu WY, Mow VC. On the conditional equivalence of chemical loading and mechanical loading on articular cartilage. J Biomechanics, In Press, 1998.
25. Fung YC, Liu SQ. Elementary mechanics of the endothelium of blood vessels. J Biomech Engng 1993;115:1–12.
26. Mow VC, Holmes MH, Lai WM. Fluid transport and mechanical properties of articular cartilage: a review. J Biomechanics 1984;17(5):377–94.
27. Gu WY, Lai WM, Mow VC. Transport of fluid and ions through a porous-permeable charged-hydrated tissue, and streaming potential data on normal bovine articular cartilage. J Biomechanics 1993;26:709–23.
28. Gu WY, Lai WM, Mow VC. A triphasic analysis of negative osmotic flows through charged hydrated soft tissues. J Biomechanics 1997;30:71–8.
29. Muir H. Proteoglycans as organizers of the intercellular matrix. Biochem Soc Trans 1983;9:613–22.
30. Hardingham TE, Fosang A. Proteoglycans: many forms and many functions. FASEB J 1992;6:861–70.
31. Poole AC. Chondrons: The chondrocyte and its pericellular microenvironment. In: Kuettner KE, et al. Eds. Articular Cartilage and Osteoarthritis. New York, NY: Raven Press 1992:201–20.
32. Aydelotte MB, Schumacher BL, Kuettner KE. Heterogeneity of articular chondrocytes. In: Kuettner KE, et al. Eds. Articular Cartilage and Osteoarthritis. New York, NY: Raven Press 1992:237–49.
33. Schinagl RM, Ting MK, Price JH, Sah RL. Video microscopy to quantitate the inhomogeneous equilibrium strain within articular cartilage during confined compression. Ann Biomed Eng 1996;24:500–12.
34. Wang CB, Mow VC. Inhomogeneity of aggregate modulus affects cartilage compressive stress-relaxation behavior (Abstract). Trans Orthop Res Soc 1998;23(1):484.

35. Guilak F, Ratcliffe A, Mow VC. Chondrocyte deformation and local tissue strain in articular cartilage. J Orthop Res 1995;13:410–21.
36. Guilak F. Compression-induced changes in the shape and volume of the chondrocyte nucleus. J Biomechanics 1995;28:1529–42.
37. Helfferich F. Ion Exchange. New York: McGraw-Hill 1962.
38. Katchalsky A, Curran PF. Nonequilibrium Thermodynamics in Biophysics. 4th ed. Cambridge: Harvard University Press 1975.
39. Donnan FG. The theory of membrane equilibria. Chemical Revs 1924;1:73–90.
40. Tombs MP, Peacocke AR. The Osmotic Pressure of Biological Macromolecules. Oxford, UK: Clarendon Press 1974.
41. Maroudas A. Balance between swelling pressure and collage tension in normal and degenerate cartilage. Nature 1976;260:808–9.
42. Urban JPG, McMullin JF. Swelling pressure of the intervertebral disc: Influence of collagen and proteoglycan content. Biorheology 1985;22:145–57.
43. Buschmann MD, Grodzinsky AJ. A molecular model of proteoglycan-associated electrostatic forces in cartilage mechanics. J Biomech Engng 1995;117:170–92.
44. Fung YC. Biomechanics: Motion, Flow, Stress and Growth. New York: Springer-Verlag 1990, Chap 11, 382–451.
45. Choung CJ, Fung YC. On residual stresses in arteries. J Biomech Engng 1986;108:189–92.
46. Setton LA, Gu WY, Mow VC, Lai WM. Predictions of the swelling-induced pre-stress in articular cartilage. In: Selvadurai APS, Ed. Mechanics of Porous Media. Kluwer Acad Press 1995:299–322.
47. Setton LA, Tohyama H, Mow VC. Swelling and curling behavior of articular cartilage. J Biomech Engng 1998;102:355–61.
48. Palmoski M, Perricone E, Brandt KD. Development and reversal of a proteoglycan aggregation defect in normal canine knee cartilage after remobilization. Arthritis Rheum 1979;22:508–17.
49. Jurvelin J, Kiviranta I, Saamanen AM, Tammi M, Helminen HJ. Indentation stiffness of young canine knee articular cartilage—influence of strenuous joint loading. J Biomechanics 1990;23:1239–46.
50. Setton LA, Mow VC, Muller FJ, Pita JC, Howell DS. Mechanical properties of canine articular cartilage are significantly altered following transection of the anterior cruciate ligament. J Orthop Res 1994;12:451–63.
51. Newton PM, Mow VC, Buckwalter JA, Albright JP. The effect of life-long exercise on canine knee articular cartilage. Am J Sp Med 1997;25:282–7.
52. Sah RLY, Kim YJ, Doong J-YH, Grodzinsky AJ, Plaas AHK, Sandy JD. Biosynthetic response of cartilage explants to dynamic compression. J Orthop Res 1989;7:619–36.
53. Sah RLY, Doong J-YH, Grodzinsky AJ, Plaas AHK, Sandy JD. Effects of compression on the loss of newly synthesized proteoglycans and proteins from cartilage explants. Arch Biochem Biophys 1991;286:20–9.
54. Parkkinen J, Lammi MJ, Helminen HJ, Tammi M. Local stimulation of proteoglycan synthesis in articular cartilage explants by dynamic compression *in vitro*. J Orthop Res 1992;10:610–20.
55. Kim YJ, Sah RL, Grodzinsky AJ, Plaas AH, Sandy JD. Mechanical regulation of cartilage biosynthetic behavior: physical stimuli. Arch Biochem Biophys 1994;311:1–12.
56. Ateshian GA, Wang H. A theoretical solution for the frictionless rolling contact of cylindrical biphasic layer. J Biomechanics 1995;28:1341–55.
57. Soltz MA, Ateshian GA. Experimental verification and theoretical prediction of cartilage interstitial fluid pressurization at an impermeable contact interface in confined compression. J Biomechanics 1998, In Press.
58. Guilak F, Bachrach NM, Mow VC. Incompressibility of the solid matrix of articular cartilage under high hydrostatic pressures. J Biomechanics 1998, In Press.
59. Lippiello L, Kaye C, Neumata T, Mankin HJ. In vitro metabolic response of articular cartilage segments to low levels of hydrostatic pressure. Conn Tissue Res 1985;13:99–107.
60. Parkkinen JJ, Ikonen J, Lammi MJ, Laakkonen J, Tammi M, Helminen HJ. Effects of cyclic hydrostatic pressure on proteoglycan synthesis in cultured chondrocytes and articular cartilage explants. Arch Biochem Biophys 1993;300:458–65.
61. Parkkinen JJ, Lammi MJ, Inkinen R, Jortikka M, Tammi M, Virtanen I, Helminen HJ. Influence of short-term hydrostatic pressure on organization of stress fibers in cultured chondrocytes. J Orthop Res 1995;13:495–502.
62. Maroudas A, Bannon C. Measurement of swelling pressure in cartilage and comparison with the osmotic pressure of constituent proteoglycans. Biorheology 1981;18:619–32.
63. Maroudas A, Bullough P, Swanson SAV, Freeman MAR. The permeability of articular cartilage. J Bone Jt Surg 1968;50B:166–77.
64. Maroudas A. Biophysical chemistry of cartilaginous tissue with special reference to solute and fluid transport. Biorheology 1975;12:233–48.
65. Mansour J, Mow VC. The permeability of articular cartilage under compressive strain and at high pressures. J Bone Jt Surg 1976;58A:509–16.
66. Lai WM, Mow VC. Drag induced compression of articular cartilage during a permeation experiment. Biorheology 1980;17:111–23.
67. Holmes MH, Lai WM, Mow VC. Singular perturbation analysis of the nonlinear, flow-dependent, compressive stress relaxation behavior of articular cartilage. J Biomech Engng 1985;107:206–18.
68. Holmes MH, Mow VC. The nonlinear characteristics of soft gels and hydrated connective tissues in ultrafiltration. J Biomechanics 1990;23:1145–56.
69. Urban JPG, Hall AC, Gehl KA. Regulation of matrix synthesis rates by the ionic environment of articular chondrocytes. J Cell Physiol 1993;154:262–70.
70. Ateshian GA, Lai WM, Zhu WB, Mow VC. An asymptotic solution for the contact of two biphasic layers. J Biomechanics 1994;27:11347–60.
71. Ateshian GA, Wang HQ, Lai WM. The role of interstitial fluid pressurization and surface porosities on the boundary friction of articular cartilage. J Tribology 1998;120:241–8.
72. Bachrach NM, Valhmu WB, Stazzone E, Ratcliffe A, Mow VC. Changes in proteoglycan synthesis of

chondrocytes in articular cartilage are associated with the time dependent changes in their mechanical environment. J Biomechanics 1996;28:1561–9.
73. Kim YJ, Bonassar LJ, Grodzinsky AJ. The role of cartilage streaming potential, fluid flow and pressure in the stimulation of chondrocyte biosynthesis during dynamic compression. J Biomechanics 1995;28:1055–66.
74. Mow VC, Ateshian GA, Lai WM, Gu WY. Effects of fixed charges on the stress-relaxation behavior of hydrated soft tissues in a confined compression problem. Int J Solid Struct 1998; 35: 4945–62.
75. Armstrong CG, Mow VC, Lai WM. An analysis of unconfined compression of articular cartilage. J Biomech Engng 1984;106:165–73.
76. Spilker RL, Suh JK, Mow VC. Effect of friction on the unconfined compressive response of articular cartilage: A finite element analysis. J Biomech Engng 1990:112:138–46.
77. Frank EH, Grodzinsky AJ. Cartilage electromechanics—I. Electrokinetic transduction and the effects of pH and ionic strength. J Biomechanics 1987;20:615–27.
78. Frank EH, Grodzinsky AJ. Cartilage electromechanics—II. A continuum model of cartilage electrokinetics and correlations with experiments. J Biomechanics 1987;20:629–39.
79. Hou JS, Holmes MH, Lai WM, Mow VC. Boundary conditions at the cartilage-synovial fluid interface for joint lubrication and theoretical verification. J Biomech Engng 1988;111:78–87.
80. Smith RL, Donlon BS, Gupta MK, Mohtai M, Das P, Carter DR et al. Effects of fluid-induced shear on articular chondrocyte morphology. J Orthop Res 1995;13:824–32.
81. Das P, Schurman DJ, Smith RL. Nitric oxide and G protein mediate the response of bovine articular chondrocytes to fluid-induced shear. J Orthop Res 1997;15:87–93.